Desalination and Water Treatment
www.deswater.com
6 (2009) 276–280

The influence of seawater temperature on the net driving force and CP degree in reverse osmosis

Sergey Agashichev*, Shamma Almalek, Abdulla Almazrouei, Elfadil Osman, Jayesh Kumar, Taher Ali, Mohammed Abdulla

National Energy and Water Research Center (ADWEA), P.O. Box 54111, Abu Dhabi, UAE
Fax +971 (2) 665 83 74; email: spagashichev@adwea.gov.ae

Received 18 December 2008; accepted 12 May 2009

ABSTRACT

The impact of temperature on net driving force and concentration polarization was considered in this study. The study is based on experimental data on permeability of reverse osmosis (RO) at different temperature. The paper contains experimental data and theoretical calculation of permeability. Elevation in temperature from $t = 20$ to $t = 35$°C is accompanied by increase of CP modulus. Experimental (and theoretical) values of CP modulus range from 1.1 (and 1.23) at $t = 20$°C to 1.2 (and 1.29) at $t = 35$°C, respectively. Satisfactory agreement between empirical data and theoretical values of CP modulus is demonstrated. Based on the analysis of the experimental performance of membrane with high degree of salt rejection, the following conclusions have been drawn: growth of temperature is accompanied by increase of hydraulic permeability of the membrane matrix itself but enhancement of surface concentration that in turn causes decline of the net driving forces. Experimental profiles are attached.

Keywords: Reverse osmosis; Concentration polarization; Impact of temperature

1. Introduction and formulation of the problem

Pressure-driven processes are accompanied by unavoidable phenomenon such as concentration polarization (CP) that is quantified by the degree of CP or polarization modulus. The impact of temperature on degree of CP and in turn on behavior of performance characteristics is essential in the analysis and the design of reverse osmosis (RO) systems [1–3]. High seawater salinity and elevated concentration of fouling factors increase sensitivity of performance characteristics to temperature. These aspects are important for implementation of RO in Gulf area, especially for the analysis of RO/MSF hybrid or integrated schemes [1,4–6]. Within the context of the problem, the objective of this study is quantifying the impact of seawater temperature on the level of CP and performance characteristics.

*Corresponding author

2. Profile of net driving force and CP modulus based on experimental data

The study is based on data produced by RO pilot system located in the United Arab Emirates (Abu Dhabi). RO elements by Toray (TM 820-370) were used (diameter: 8″; membrane area: 34 m^2; number of elements: 7). Further analysis is based on the following assumptions: gel-enhanced CP is outside the scope of the study, morphology of membrane matrix is temperature independent. Experimental data on seasonal variation of seawater temperature and permeability at operating temperature are shown in Figs. 1 and 2.

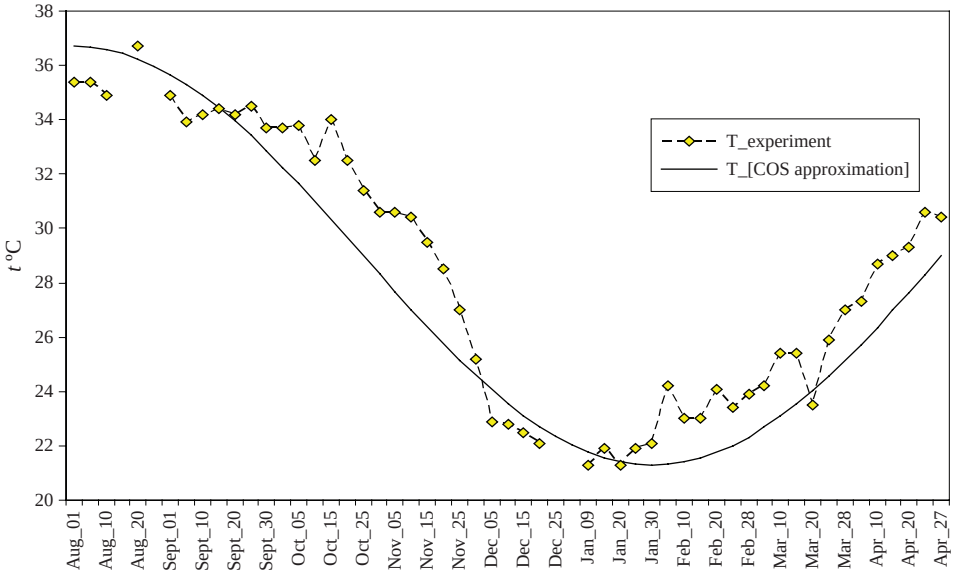

Fig. 1. Seasonal variation of temperature.

Experimental permeability at operating temperature remains almost constant throughout the year. It is maintained by adjustment of operating pressure. It is linked to the driving force through specific membrane permeability $A_M(t)$ as:

$$V_M(t,\alpha) = A_M(t)[\Delta P - \pi_M(t)] \quad (1)$$

Being multiplied by the viscosity-correction factor, $\mu(t)\big/\mu_{(t0)}$, it gives the operating permeability normalized at reference temperature. The sinusoidal-shape profile is shown in Fig. 2. The shape of the corrected profile is in correspondence with the seasonal behavior of temperature. Hydraulic membrane permeability at operating temperature (membrane constant) is related to the permeability at the reference temperature as $A_M(t) = A_{M(t0)}\mu_{(t0)}\big/\mu(t)$. Inserting $A_M(t)$ into Eq. (1) we get the net driving force, $\Delta P - \pi_M(t)$, against operating temperature:

$$[\Delta P - \pi_M(t)] = V_M(t,\alpha)\mu(t)\big/A_{M(t0)}\mu_{(t0)} \quad (2)$$

where π_M, osmotic pressure at the membrane surface,

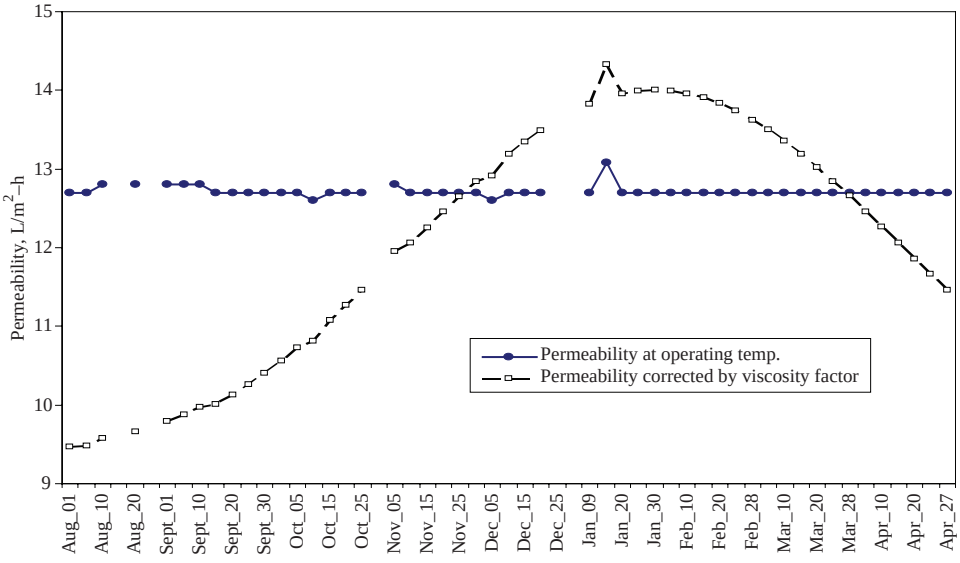

Fig. 2. Experimental profiles of permeability at operating temperature and permeability normalized at the reference temperature, $t_0 = 25°C$ (applied operating pressure ranges from $P = 60$ to $P = 65$ bar).

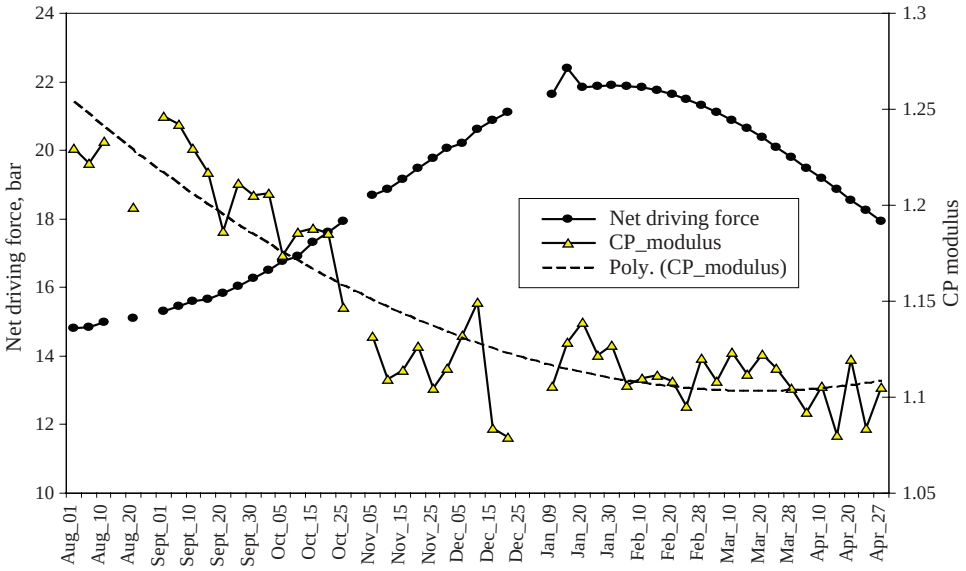

Fig. 3. Net driving force and CP modulus (these profiles are based on experimental data of normalized permeability).

$$\pi_M = i\alpha(t)C_1RT \tag{3}$$

Combining Eqs. (2) and (3) we get the CP modulus against operating temperature:

$$\alpha = \left[\Delta P - V_M(t,\alpha)\mu(t)\Big/A_{M(t0)}\mu_{(t0)}\right]\Big/[iC_1R(273+t)] \tag{4}$$

Profiles of net driving force and CP based on experimental data on permeability $V_M(t,\alpha)$, operating pressure, ΔP and temperature, t are shown in Fig. 3.

3. Comparison of experimental and calculated data

Experimentally-based profiles were compared with theoretical calculations of the CP modules. The following expression for the concentration profile was proposed in the previous study [7,8].

$$C(\eta)/C_1 = \exp\{V_M(t)H[X(\eta,t) - Z(f,t)]/D(t)\} \tag{5}$$

At $\eta = 1$ Eq. (5) gives the CP modulus at the membrane surface

$$\alpha_{(\eta=1)} = (C_{1M}/C_1)_{\eta=1} = \exp\{V_M(t)H[X(t) - Z(f,t)]/D(t)\} \tag{6}$$

where

$$X(\eta,t) = 0.75\eta^2 - 0.125\eta^4 - \eta + A(\alpha,f)[B(\alpha,f)]^{-1} \exp[B(\alpha,f)\eta] \tag{7}$$

$$Z(f,t) = 0.75f^2 - 0.125f^4 - f + A(\alpha,f)[B(\alpha,f)]^{-1} \exp[B(\alpha,f)f] \tag{8}$$

$$A(\alpha,f) = R_{TRUE}\Big/\sqrt[f-1]{R_{ORSERVED}/R_{TRUE}} \tag{9}$$

$$B(\alpha,f) = \ln(R_{OBSERVED}/R_{TRUE})/(f-1) \tag{10}$$

Impact of temperature was accounted through temperature-dependence of physical properties namely: viscosity $\mu(t)$, diffusivity $D(t)$, Sc number $Sc(t)$, thickness of diffusion layer $f(t) \approx Sc(t)^{-1/3}$ [9–10], and intermediate parameters of Eq. (6) such as $A(f,\alpha)$. $B(f,\alpha)$, $X(\eta,t)$, $Z(f,t)$ and so on. Simplified flowchart based on sub-model for concentration profile is shown in Fig. 4. Impact of temperature on experimental and theoretical projection of polarization modulus (C_{1M}/C_1) is shown in Fig. 5.

Variability of experimentally-based CP module was characterized by means of true standard deviation $\sigma(\alpha)$ as follows:

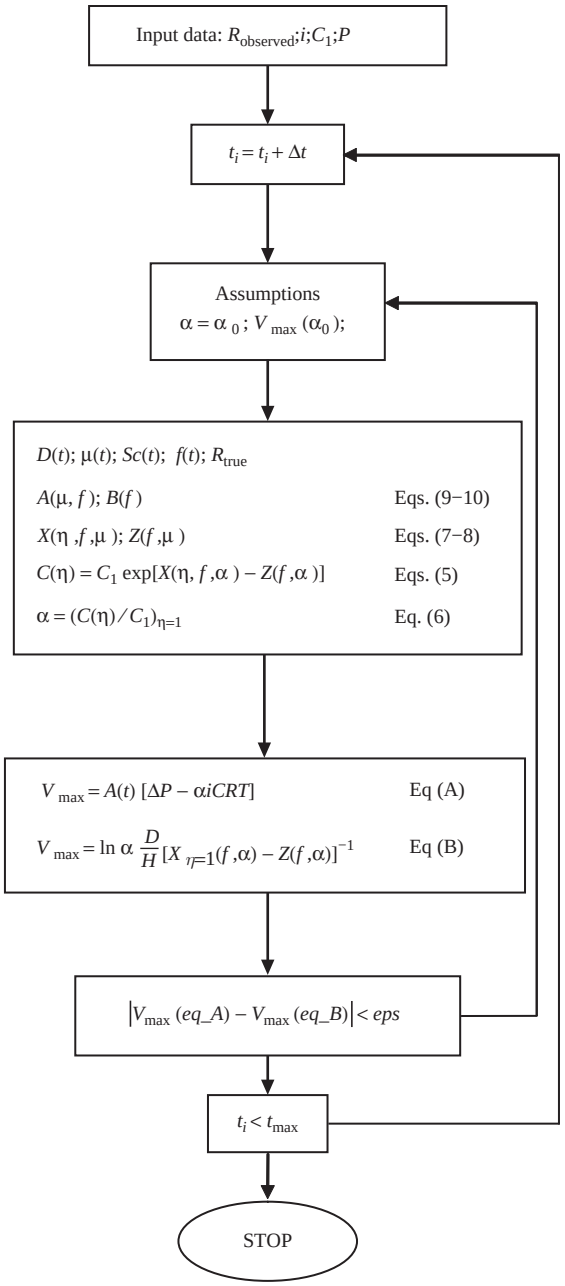

Fig. 4. Simplified flowchart of the algorithm.

$$\sigma(\alpha) = \sqrt{\frac{\sum(\alpha_i - \alpha)^2}{n}} \tag{11}$$

It was estimated to be $\sigma(\alpha) = 0.02554$. Average difference between experimental and model values does not exceed 12%.

4. Conclusions

Based on analysis of experimental data and calculated results the following conclusions have been drawn:

1. Growth of temperature causes growth of surface concentration and CP degree at membrane surface.
2. Growth of temperature is accompanied by increase of the hydraulic permeability of membrane matrix itself and decline of net driving forces.
3. Correspondence between calculated and experimental profiles is observed. (Estimated standard deviation of experimentally-based CP module is to be $\sigma(\alpha) = 0.02554$. Average difference between model and experimental values do not exceed 12%.

Acknowledgement

The authors are grateful to the National Energy and Water Research Center (ADWEA) for supporting this study.

Symbols

$A_M(t)$	hydraulic permeability of membrane, m^3/m^2 s bar
C	concentration, mol/m^3, kg/m^3, ppm
D	diffusion coefficient, $m^2\ s^{-1}$
f_C	coordinate of upper boundary of diffusion layer, dimensionless
H	channel half-height, m
m	number of observations
P	operating pressure, bar
T	temperature, K
$R_{M(OBSERVED)}$	observed degree of rejection, $R_{M(OBSERVED)} = (C_1 - C_2) / C_1$, dimensionless
$R_{M(TRUE)}$	true degree of rejection, $R_{M(TRUE)} = (C_{1M} - C_2) / C_{1M}$, dimensionless
V	transmembrane or transverse velocity, m/s
α	CP modulus, $\alpha = C_{1M}/C_1$ dimensionless
μ	apparent viscosity of fluid, Pa s
ρ	density, kg m^{-3}
Π	osmotic pressure, bar
Sc	Schmidt number, $Sc = \mu/D\rho$

Subscripts

1	identifies parameter corresponding to the bulk of solution
1M	identifies parameter corresponding to membrane surface

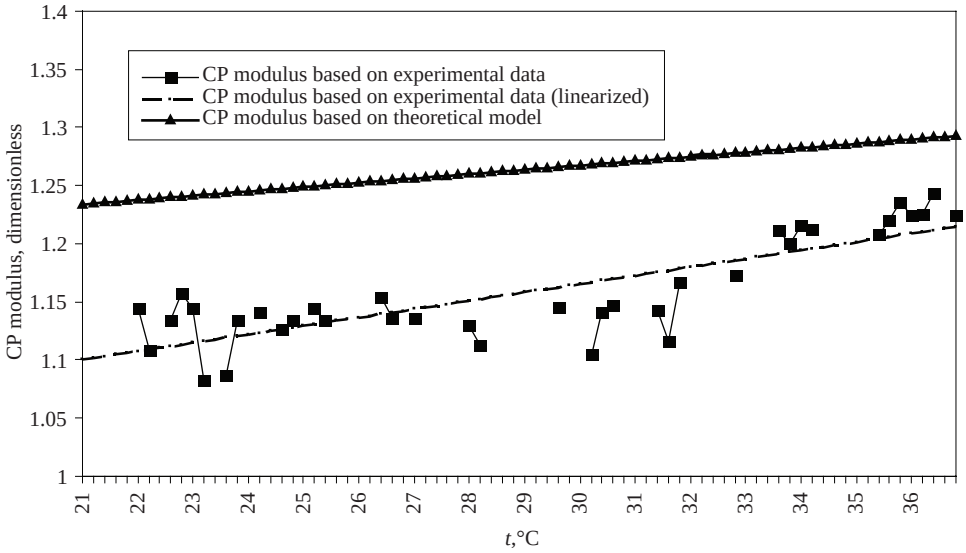

Fig. 5. mpact of temperature on experimental and theoretical projection of the polarization modulus (C_{1M}/C_1). Theoretical profile is based on Eq. (6).

LONG corresponds to longitudinal sub-constituents
t_0 reference temperature, $t = 25$

References

[1] M.R. Al-Marafie, Prospects of hybrid RO/MSF desalting plants in Kuwait, Desalination, 72 (1989) 395-404.
[2] L. Awerbuch, Power-desalination and importance of hybrid ideas, in: IDA World Congress on Desalination, vol. 4, Spain, 6–9 October, 1997, pp. 184-192.
[3] B.A. Kamaluddin, J.L. Talavera and K. Wangnik, Reverse osmosis seawater desalination systems in co generation plants for additional production of drinking water using off-peak electrical energy, in: IDA World Congress on Desalination, vol. 1, Spain, 6–9 October, 1997, pp. 387-413.
[4] K. Wangnik, A global overview of water desalination technology and the perspectives, in: International Conference on Spanish Hydrological Plan and Sustainable Water Management (Environmental Aspects, Water Reuse and Desalination), Zaragossa, Spain, 13–14 June, 2001.
[5] Z.K. Al-Bahri, W.T. Hanbury and T. Hodgkiess, Optimum feed temperature for seawater reverse osmosis plant operation in an MSF/SWRO hybrid plant, Desalination, 138 (2001) 335-339.
[6] R. Humphries, K. Davies and J. Ackert, Nuclear desalination using preheated feed water: an advanced RO system coupled with a CANDU nuclear reactor, in: IDA World Congress on Desalination and Water Reuse, Manama, Bahrain, 8–13 March, 2002.
[7] S.P. Agashichev and K.N. Lootah, The influence of temperature and permeate recovery on energy consumption of a reverse osmosis system, Desalination, 154 (2003) 253-266.
[8] S.P. Agashichev, Modeling the influence of temperature on resistance of concentration layer and transmembrane flux in reverse osmosis system, Separat. Sci. Technol., 39(14) (2004) 3215-2336.
[9] R.H. Perry, D.W. Green, eds., Perry's Chemical Engineers' Handbook, 6th ed., McGraw-Hill, New York, 1984.
[10] H. Schlichting, Grenzschicht-Theorie, 5th ed., Verlag G. Braun, Karlsruhe, 1974.